Novel 100 GHz GaAs/AlGaAs MQW IMPATT Oscillators :p^+n Single-Drift Structures on p^+ Substrates

C. C. Meng#, S. W. Siao and H. R. Fetterman
Department of Electrical Engineering
University of California, Los Angeles
Los Angeles, CA 90024

D. C. Streit, T. R. Block and Y. Saito
TRW
Space & Electronics Group
Redondo Beach, CA 90278
Currently working at Avantek/Hewlett Packard

I Introduction

We have successfully fabricated and tested GaAs/$Al_{0.3}Ga_{0.7}As$ MQW (Multiquantum Well) IMPATT (IMPact ionization Avalanche Transit Time) oscillators at 100 GHz. For the first time to our knowledge, CW operation of MQW IMPATT devices at 100 GHz has been achieved. Conventional GaAs IMPATT devices show a fall-off in efficiency at the frequencies above 50 GHz because of the saturation of the ionization rates at high electric fields. Recently, MQW structures have been proposed to reduce the ionization rate saturation limitations[1]-[3]. Efficiencies of 13% at 100 GHz and 10% at 140 GHz were projected for GaAs/AlGaAs single-drift flat-profile MQW IMPATT devices[3]. Preliminary results yielded 6.4 mW CW power at 100.3 GHz and 364 mA bias current in a non-optimized circuit. Experimental efforts are underway to optimize the circuit parameters and significantly higher powers are anticipated.

II Impact Ionization in MQW Structures

Ionization rate saturation limitations occur when an IMPATT device is biased at high electric fields for high frequency operations. The saturation of ionization rates at high electric fields results in a broaden injected current pulse in a less localized avalanche region and degrades the device efficiency[4]. The ionization rate saturation limitations can be reduced by replacing the bulk avalanche region by a GaAs/AlGaAs MQW structure. Impact ionization is characterized by an ionization threshold energy. A wider bandgap material has a higher impact ionization threshold energy and the ionization rate at any given electric field has an exponential dependence on the ionization threshold energy. Consider the case of a GaAs/AlGaAs multiquantum well structure. We use E_T for bulk GaAs ionization threshold energy and E_{TA} for bulk AlGaAs ionization threshold energy. When electrons (holes) enter the barrier region of a multiquantum well structure, electrons (holes) lose

some kinetic energy to the band discontinuity and thus the effective threshold energy (E'_{TA}) becomes higher higher. Here E'_{TA} can be expressed as $E'_{TA} = E_{TA} + \Delta E$, where ΔE is the band offset energy. The probability of impact ionization in the barrier region is reduced. If the barrier length is designed to be comparable to the energy relaxation length, then electrons (holes) can obtain energy when traveling through the barrier region. When an electron (hole) exits the barrier and enters the well, it sees a less effective threshold energy (E'_T) in the well region. E'_T can be expressed as $E'_T = E_T - (\Delta E + e\xi l_{eff})$. Here $e\xi l_{eff}$ is the energy obtained from the potential barrier, where l_{eff} is the effective energy acceleration length and is equal to the smaller value of the two quantities, (1) energy relaxation length and (2) barrier length.

Because E'_{TA} is much larger than E'_T, we can assume that impact ionization is forbidden in the barrier region and E'_T can be treated as the threshold energy for the whole multiquantum well structures. The amount of reduction in E'_T becomes higher at higher electric field and thus the amount of increase in the ionization rate also becomes higher at higher electric field. Thus, a multiquantum well structure can improve the nonlinearity of the avalanche process and reduce the ionization rate saturation limitations.

III Structure Design & Device Characteristics

The band diagram for the designed single-drift flat profile MQW IMPATT is shown in figure 1. The structure is a p^+n junction with five periods of MQWs (100$\AA$ barrier length and 100$\AA$ well length) in the avalanche region. The transit time drift region is 1500$\AA$ thick and the corresponding transit time angle is 0.75 π at 100 GHz when the electron saturation velocity is 4×10^6cm/sec. Doping density in the multiquantum well region is not constant. In an MBE system, n-type dopant replaces both Al and Ga atoms when Al flux is introduced during growth. Thus, the doping density is lower in AlGaAs layer for the simple growth condition of a constant Si flux rate in an MBE system. This problem can be circumvented by using two Si dopant guns or by using growth interruption to raise the Si flux rate in AlGaAs layers to compensate for this extra Al. However, an IMPATT structure can definitely tolerate deviation from the mean doping density to some degree. Therefore, the active layer doping densities of $2 \times 10^{17}/cm^3$ for GaAs layers and $1.4 \times 10^{17}/cm^3$ for $Al_{0.3}Ga_{0.7}As$ layers were designed for the simple growth condition of a constant Si flux rate in an MBE system.

The room temperature I-V curve in figure 2 for the structure in figure 1 shows the desired hard breakdown at 10 V. A 7 V punch through voltage was obtained from a C-V measurement and agrees well with the designed structure. From both I-V and C-V measurements, the device has at least 30% voltage amplitude modulation if the punch through voltage is taken to be the minimum voltage when the device oscillates.

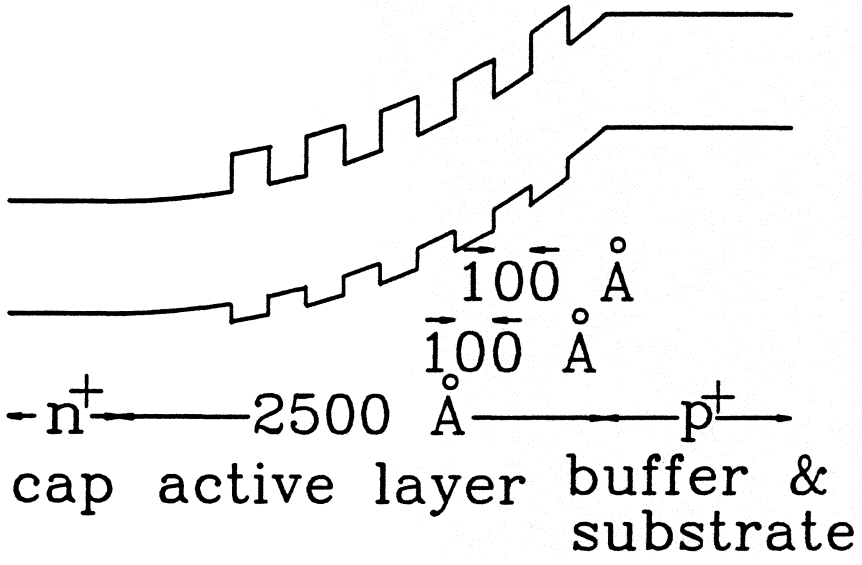

Figure 1: The band diagram of a GaAs/AlGaAs MQW IMPATT device on a p^+ GaAs substrate.

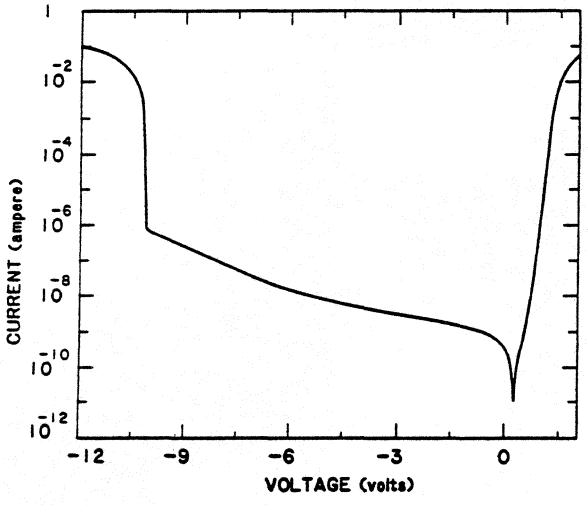

Figure 2: Room I-V curve for the GaAs/AlGaAs MQW IMPATT structure.

IV Substrate Selection and its Effect on Edge Breakdown

The structure as shown in figure 1 was grown on a p^+ GaAs substrate in an MBE system. Figure 3 illustrates a diagram of the high frequency diode on a heat sink. The p^+ substrate plays an important role in device edge breakdown. The band diagram of a GaAs/AlGaAs multiquantum well IMPATT device on a p^+ GaAs substrate was illustrated in figure 1. Because IMPATT devices are normally flip-chip mounted to dissipate heat efficiently, the edge slope of the diode mesa in figure 3 results in the equi-potential lines bending towards the p^+n junction. The band diagram near the edge (the area enclosed in a dotted square box in figure 3) is illustrated in figure 4. Because quantum wells can trap and release carriers in a dynamic way, the band bending near the edges will keep trapped holes away from the edges and push trapped electrons towards the edges. Thus, the lower effective doping near the edge makes the edge breakdown voltage to be higher and prevents early edge breakdown. On the other hand, if the p^+n multiquantum well IMPATT structure is grown on a n^+ substrate, the effective doping density at edges becomes higher when the device is biased at higher current and the lower edge breakdown voltage can cause early device failure. Because of the edge breakdown consideration, we used a p^+ substrate for the designed p^+n MQW IMPATT structure.

V Device Fabrication & Device Packaging

High frequency high power devices generate tremendous heat and are susceptible to the parasitic effects. However, semiconductors have poor thermal conductivity. Thus a flip chip mounting configuration with the junction side close to a good heat sink is used. A low parasitic quartz ring is used for device package. The tiny quartz ring requires a small device die size which is difficult to obtain by dicing. Also the resistance caused by the remaining substrate is enhanced by the skin effect at high frequencies. Thus, a novel wafer-thinning and device-separating fabrication technique has been developed to fabricate the MQW IMPATT devices.

Circular AuGe/Ni/Au metal patterns and mesas were defined on the epitaxial side of the wafer by a conventional photolithography technique. A thick layer of silver (75μm) was electroplated on the epitaxial side of the wafer before the wafer was chemically thinned down from the substrate side to facilitate the handling of this thin wafer for the rest of the fabrication process. After the wafer was chemically thinned down, circular AuGe/Ni/Au metal patterns and mesas were then also defined on the substrate side of this thin wafer. The devices were alloyed and separated by chemical etching. A diode after the separating step is 10μm thick and has AuGe($900\mathring{A}$)/Ni($150\mathring{A}$)/Au(1μm) on both sides.

The diode is T.C. bonded on a diamond heat sink and then packaged inside a 5 mil thick quartz ring (18 mil inner diameter and 30 mil outer diameter). A triple-strap ribbon connects one end of the diode to the quartz ring. The center of the triple-strap ribbon is tapered down to 2 mil to facilitate the ribbon bonding. Figure 5 illustartes the dimensions

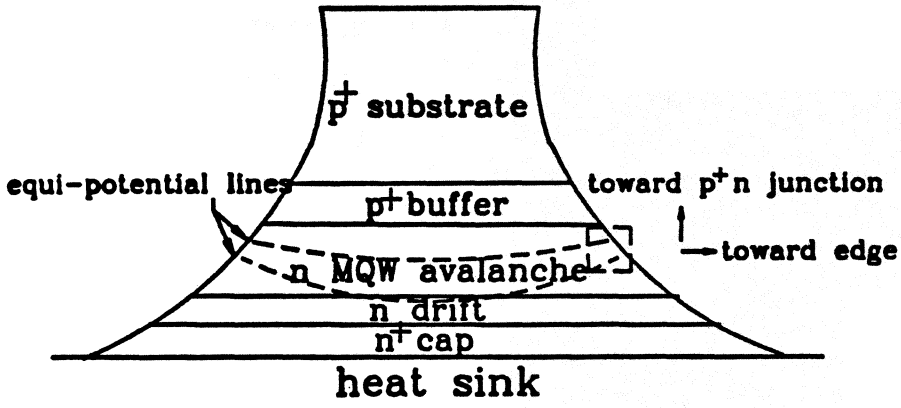

Figure 3: A flip-chip mounted GaAs/AlGaAs MQW IMPATT diode with p^+ GaAs substrate on a heat sink.

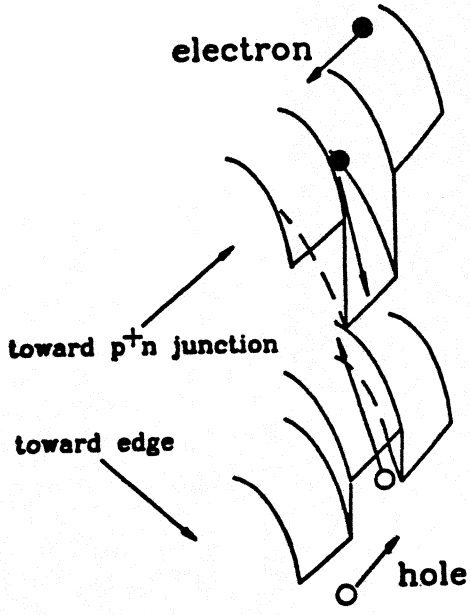

Figure 4: The band diagram near the edge (the area enclosed in a dotted rectangular box in figure 3) of a MQW IMPATT device.

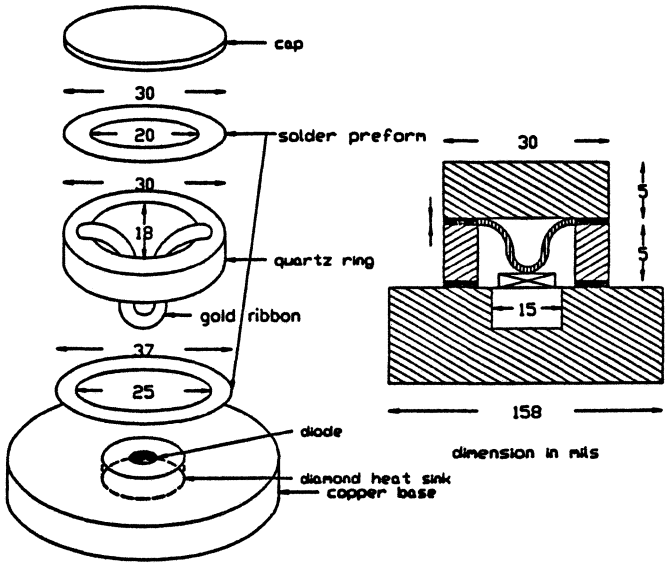

Figure 5: Dimensions for the quartz ring package.

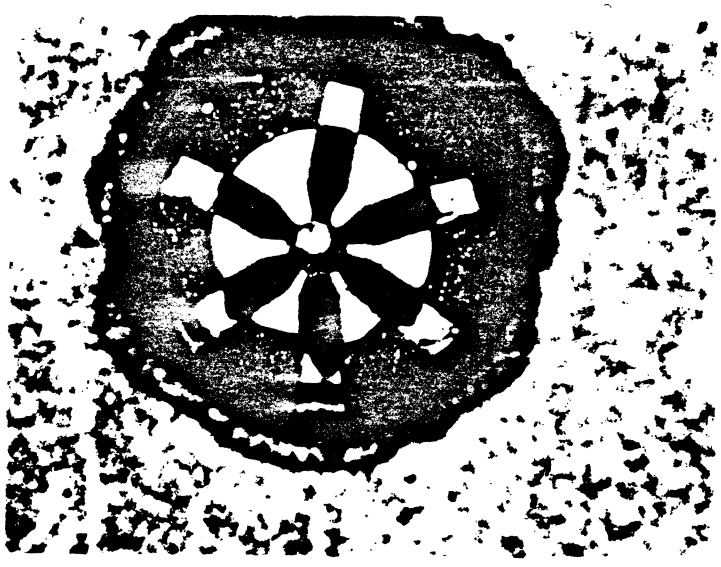

Figure 6: The picture of a triple-strap quartz ring package.

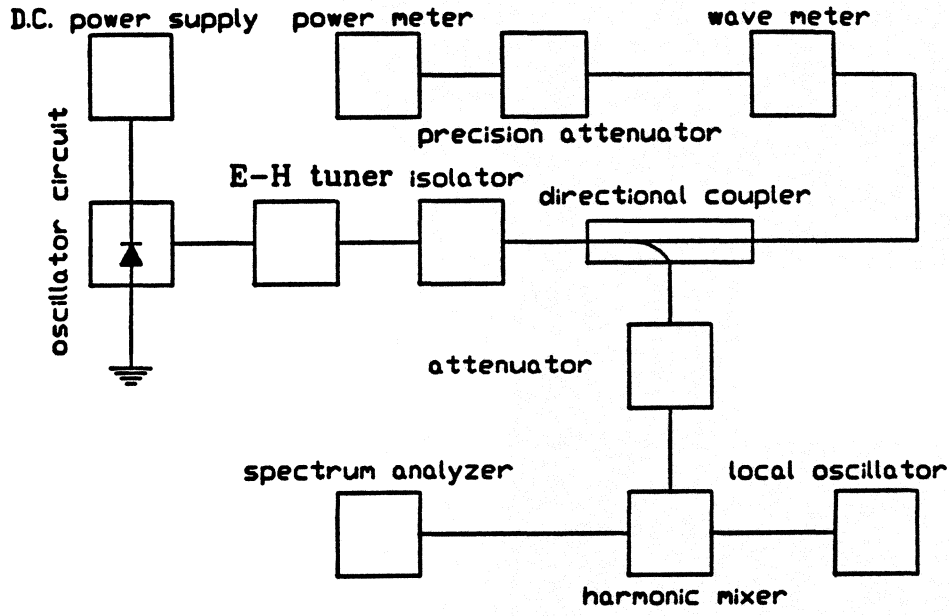

Figure 7: Measurement set-up for the W-band MQW IMPATT oscillator.

for the quartz ring package and figure 6 shows the picture of the quartz ring package. Inside the package the ribbon prevents the top contact metal from shorting to the ground, the device area is adjusted by the trim procedure to have approximate 1 pf at zero bias for r.f. testing.

VI Measurement Results and Discussions

The W-band (75-110 GHz) high frequency measurement set-up is shown in figure 7. The oscillator circuit is a Kurokawa-type oscillator circuit in a reduced waveguide. An E-H tuner was placed after the oscillator circuit to optimize the device-circuit impedance matching. The spectrum of an oscillator was measured by a heterodyne detection technique and figure 8 shows the spectrum of a CW MQW IMPATT oscillator at 101.3 GHz. Oscillation frequency and r.f. power can be directly read from a wavemeter and a calibrated thermistor power meter. CW oscillation at 100.3 GHz has been obtained with 6.4 mW at 364 mA bias current for a diode under test and the output power and oscillation frequency as a function of the bias current is illustrated in figure 9. Devices tested in a pulsed mode showed oscillation at 94 GHz with power of 127 mW and 2.2% efficiency.

No attempt has been made to optimized the device-circuit impedance and with further

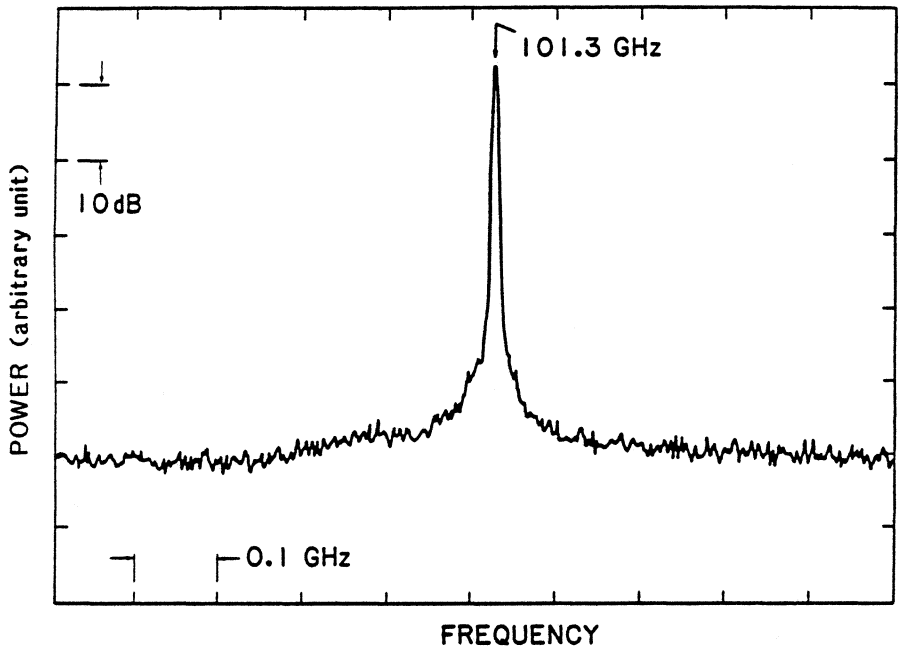

Figure 8: Spectrum of the CW MQW IMPATT diode at 101.3 GHz; the resolution bandwidth is 3 MHz.

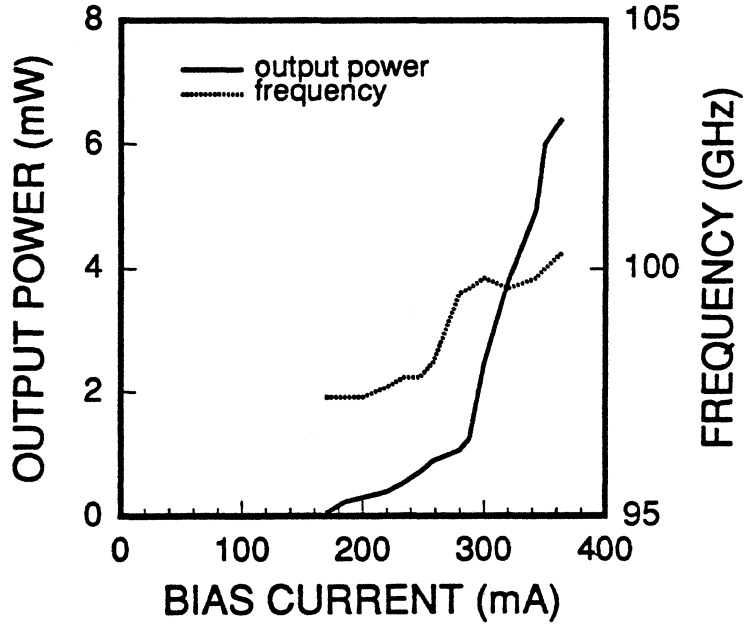

Figure 9: Output power frequency as a function of bias current for a CW MQW IMPATT oscillator.

improvement in impedance matching higher powers are expected. Also, the series resistance caused by the remaining substrate can be further minimized. The wafer-thinning technique developed can thin down the device to $1.5\mu m$ thick and a $10\mu m$ device thickness was chosen to facilitate device packaging. A device with $1.5\mu m$ thick can be packaged with further optimization in the bonding pressure, bonding temperature and bonding time. A p^+ substrate has higher ohmic loss than an n^+ substrate. A careful design on the well length, barrier length and barrier height could reduce the dynamic trapping behavior of the quantum wells at the operating current and thus an n^+ substrate can be used. Certainly, a double-drift structure with the MQW structure incorporating only into the p side can be grown on an n^+ substrate and complies with the edge breakdown consideration.

In summary, the performance of GaAs/$Al_{0.3}Ga_{0.7}$As MQW IMPATT devices at W-band frequencies was described. The operation of GaAs/AlGaAs MQW IMPATT devices at frequencies around 100 GHz opens up a new field for many millimeter-wave applications by bringing the modern epitaxy technologies to two terminal high frequency sources.

ACKNOWLEDGEMENT

This work was supported in part by the Air Force Office of Scientific Research under the direction of H. R. Schlossberg.

REFERENCES

[1] D. Lippens, O. Vanbesien and B. Lambert, " Multiquantum well GaAs/AlGaAs structures applied to avalanche transit time devices," *Journal De Physique, Vol. C5, pp. 487-290, 1987.*

[2] C. C. Meng and H. R. Fetterman, "Multiquantum well IMPATT devices in W-band frequencies," *International Semiconductor Device Research Symposium, pp. 79-82, 1991.*

[3] C. C. Meng and H. R. Fetterman, "A theoretical analysis of millimeter-wave GaAs/AlGaAs multiquantum well transit time devices by the lucky drift model," *Solid-State Electron., Vol. 36, No. 3 pp. 435-442, 1993.*

[4] T. Misawa, "High-frequency fall-off of IMPATT diode efficiency," *Solid-State Electron., Vol. 15, pp. 457-465, 1972.*